Journal of Radioanalytical and Nuclear Chemistry (2023) 332:3047–3058
https://doi.org/10.1007/s10967-023-08972-8

Determination of natural radioactivity and the associated radiation hazards in beach sediments along the North Chennai to Pondicherry coastal area, India

V. Sathish[1] · A. Chandrasekaran[1]

Received: 17 February 2023 / Accepted: 19 May 2023 / Published online: 29 May 2023

Abstract
In this study, 21 sediment samples were collected from twenty-one locations along the North Chennai to Pondicherry coastal area, India to estimate the activity concentration of ^{238}U, ^{232}Th, and ^{40}K using a NaI(Tl) γ-ray detector. The average activity concentrations for ^{238}U, ^{232}Th, and ^{40}K are 50, 32, and 543 Bq kg^{-1}, and the mean value of radiological parameters like dose rate (124 nGy h^{-1}), excess lifetime cancer risk (0.53×10^{-3} mSvy^{-1}), and annual gonadal dose equivalent (457 μSv y^{-1}) are exceeds the world permissible limit. Pearson correlation analysis was performed on the radiological variables to understand the relation between them.

Keywords Sediment · NaI(Tl) γ-ray detector · Absorbed dose rate · Pearson correlation

Introduction

In an environment, human beings are harmed by radiation from three types of isotopes: radioactive isotopes (naturally occurring isotopes of the earth's crust), cosmogenic isotopes, and manmade isotopes [1, 2]. Particularly, in natural radioisotopes, the uranium series originates from ^{238}U, the thorium series originates from ^{232}Th, and the actinium series originates from ^{235}U. There is most important singly occurring radionuclide is ^{40}K because it is a gamma-ray emitter in addition to beta decays and therefore contributes significantly to gamma radiation exposure [3]. Exposure of ionizing radiation to humans is due to the presence of a significant amount of natural radionuclides ^{238}U, ^{232}Th, and ^{40}K and their progenies in the environmental matrix such as soil, sediment, rock, water, etc. The concentration of these radionuclides is enhanced along the coastal area due to natural activities such as the leaching from parent rocks through both erosion and dissolution and anthropogenic activities such as nuclear accidents, nuclear weapons, mining, fertilizers derived from phosphate rock, drilling, transportation, and burning of fossil fuels [4, 5]. Such an enhanced activity concentration (monazite-bearing sands) was identified along the east coastal zones of India namely Orissa, Tamil Nadu, and Kerala.

In the coastal area, sediments are inorganic silicon-rich coarse materials that are derived from weathering of parent rocks. They may have deposited to their place after transport by winds, rivers, and glaciers due to the actions of waves and currents [6]. Also, mineral tracers are deposited and distributed throughout the beach during rainfall and tsunamis. This causes the accumulation of radioactive minerals and hence natural radioactivity increases in the area [7]. The coastal area has attracted all types of people across the world. With high accessibility, people settle on the coasts to live as well as leisure, recreational activities, and tourism [8]. Assessment of natural radioactivity is the most important work towards the health concern because it could cause some health issues such as bone, liver, lung, and breast cancers, anemia, and cataracts [9, 10]. Especially, cancer tissues are introduced into the human body by exposure to gamma radiation from ^{238}U, ^{232}Th, and ^{40}K. For these reasons, there is a need to measure and monitor the natural radioactivity along the coastal area. Recently, many potential researchers have carried out extensive work on the natural radioactivity level on beaches across the world [11–23], while the data

✉ A. Chandrasekaran
chandrasekarana@ssn.edu.in

[1] Department of Physics, Sri Sivasubramaniya Nadar College of Engineering (Autonomous), Kalavakkam, Chennai 603 110, India

about the natural radioactivity of beach sand along the North Chennai to Pondicherry coastal area, India is not available. A few regions of India's western coast are also high in natural radioactivity, while the country's southeast coast is known as one of the locations with the highest natural background radiation levels around the world. Despite the abundance of studies conducted around the world, there is a scarcity of radionuclide research on the North Chennai to Pondicherry coastal area. Therefore, the current investigation focused on radioactivity in coastal sediments because it might have a very large background level due to geology of the location. Hence, the main objectives of the present work are (i) to determine the activity concentration of radionuclides (^{238}U, ^{232}Th, and ^{40}K) in the North Chennai to Pondicherry coastal sediments by NaI(Tl) gamma-ray spectrometry, (ii) to assess the radiological risks in coastal sediments by calculating the radium equivalent activity (Ra_{eq}), gamma dose rate (D_R), annual effective dose equivalent (AEDE), external hazard index (H_{ex}), excess lifetime cancer risk (ELCR), annual gonadal dose equivalent (AGDE), (iii) to assess the relationship between the radioactive variables using Pearson correlation analysis.

Study area

The sprawling study area of ~160 km in length was surveyed along the North Chennai to Pondicherry coastal area for sample collection. The sampling points along the study area are shown in Fig. 1. The cumulative study area spread from Kalanji (13°19′8.94″N; 80°20 ′ 33.7554″E) Thiruvallur district of Tamil Nadu to Kalapet (12°0′53.496″N; 79°51′41.1474″E) near Pondicherry university at Pondicherry. This area covers mainly 4 coastal districts of Tamil Nadu such as Tiruvallur, Chennai, Chengalpattu, and Villupuram. During the last few decades, the study area is fully dominated by tourism, transportation, seaports, urbanization, industry, and aquaculture activities. It also covers some famous beaches like Mahabalipuram Beach (A historical place), Edward Elliot's Beach, and Marina Beach (2nd longest urban beach in the world) which is visited by many tourists [24, 25] from across the world, and also has an active atomic power station. The Palar River runs into the Bay of Bengal at Vayalur, approximately 70 km south of Chennai (near the Indira Gandhi Centre for Atomic Research–IGCAR, Kalpakkam) [26]. Thus, the study area pays more attention to measuring the level of radiation exposure due to the presence of natural radionuclides.

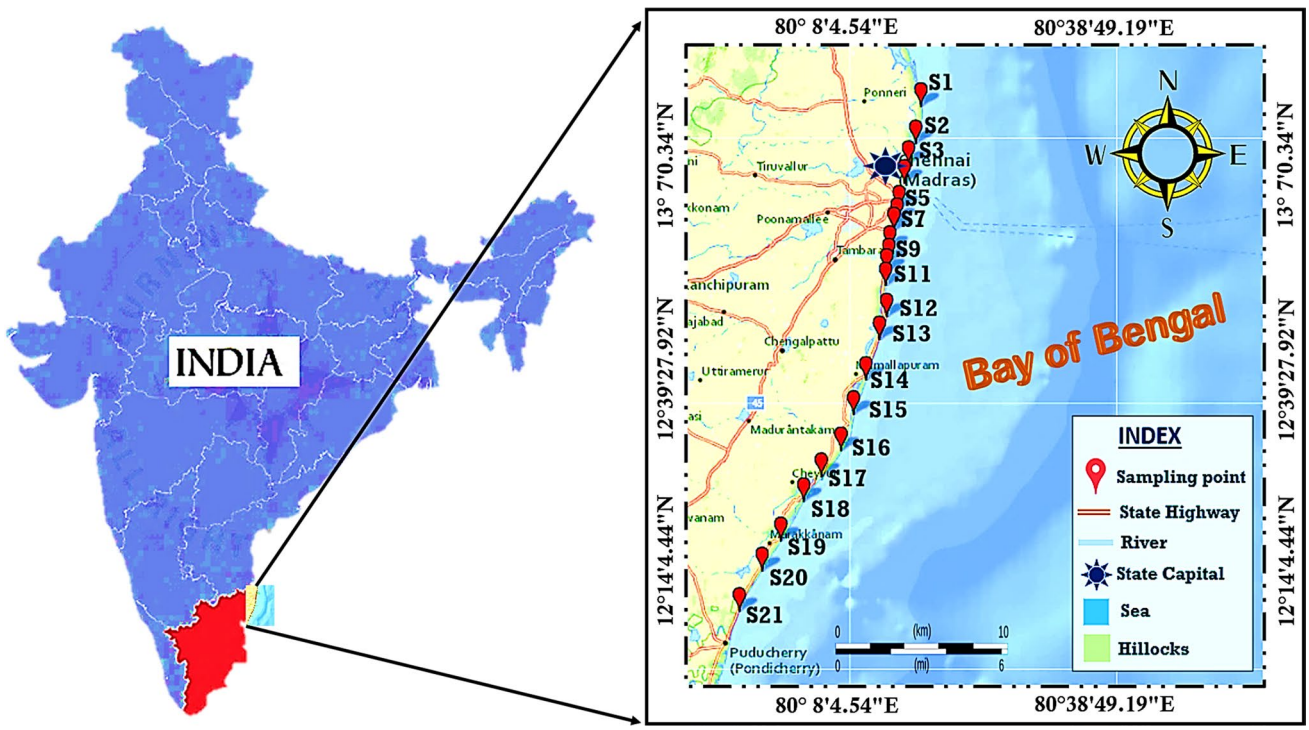

Fig. 1 A map of the North Chennai to Pondicherry, India (Study area) showing the sampling points

Experimental methods

Sample collection and preparation

The 21 sediment samples were collected from twenty-one locations along the North Chennai to Pondicherry coastal area, India (from the period March–July 2022). The sampling pathway covers an interval of 5–10 km for urban coasts and 10–15 km for non-urban coasts. The geographical coordinates of each location were noted using a hand-held Garmin global positioning system and given in Table 1. Each location was 0–20 m away from the high tide and (Fig. 1), about 2 kg of sediment samples were collected at 40 cm depth from the surface level using a stainless-steel T-rod mud auger [27]. The collected samples were placed in polythene covers and properly labelled and transported to the laboratory.

Other unwanted substances like stones, shells, pebbles, and macro impurities present in sediment samples were completely removed. In order to obtain a constant weight, samples were allowed to dry under direct sunlight, and also each sample was oven-dried at 110 °C for 2 h to remove the moisture content. Before radionuclides measurements, samples are mashed, dehydrated, and sieved, then samples were tightly stuffed with a radon-impermeable 250-cc volume of trap-shaped polyethylene containers with uniform size (dia: 60 mm; height: 120 mm) and hermetically sealed for 2 fortnights to reach secular equilibrium between ^{238}U, and ^{232}Th series and their respective progenies [28, 29]. It was assumed ^{222}Rn, and ^{220}R could not escape from the containers.

γ-ray spectrometry

The gamma-ray spectrometry equipment at the sophisticated "Radiation physics laboratory" in the Department of Physics, Sri Sivasubramaniya Nadar College of Engineering, Chennai, India, was used for this research. A gamma-ray spectroscopy system consists of a Sodium Iodide Thallium (NaI-Tl) scintillation detector with a 98% effectiveness in counting which is paired with a 1024-channel computerized multi-channel analyzer (MCA). A (NUCLEONIX, GR611M) detector with Anuspect (version 1.0) software was employed for these measurements, with a resolution for the energy of FWHM is 3.398 keV at 1332 keV of gamma line for ^{60}Co. The detector and pre-amplifier were placed inside a lead shield containing an inner concentric cylinder of Cu foils (0.3 mm) to absorb X-rays generated in the lead [28]. This entire structure was contained under a 15 cm squared lead shield to minimize ambient noise in the system. For efficiency calibration, the approved Standard International Atomic Energy Agency (IAEA) sources of reference-grade materials such as RG-U (4940 ± 30 Bq kg^{-1}), RG-Th (3250 ± 90 Bq kg^{-1}), and RG-K ($14{,}000 \pm 400$ Bq kg^{-1}) were used [30–32]. The energy calibration was accomplished by

Table 1 Geographical co-ordinates of the sampling locations along the study area

Sl. No	Sampling locations	Sample ID	Latitude	Longitude
1	Kalanji Beach	S1	13°19′8.94″N	80°20′33.76″E
2	Thazhankuppam Beach	S2	13°13′24.08″N	80°19 ′ 42.01″E
3	Thiruvottiyur Beach	S3	13°10′9.70″N	80°18′40.86″E
4	Kasimedu Beach	S4	13°7′22.37″N	80°18′1.40″E
5	Marina Beach	S5	13°3′17.71″N	80°17′5.28″E
6	Besant Nagar Beach	S6	12°59′52.84″N	80°16′21.18″E
7	Pattinapakkam Beach	S7	13°1′28.56″N	80°16′44.58″E
8	Neelankarai Beach	S8	12°56′5.61″N	80°15′42.16″E
9	Injambakkam Beach	S9	12°55′7.68″N	80°15′21.53″E
10	Panaiyur Beach	S10	12°53′31.27″N	80°15′12.85″E
11	Kanathur Beach	S11	12°51′28.15″N	80°14′57.95″E
12	Semmanchery Kuppam Beach	S12	12°46′35.90″N	80°15′11.88″E
13	Nibav Beach	S13	12°43′0.88″N	80°13′54.95″E
14	Mahabalipuram Beach	S14	12°36′0.33″N	80°11′53.63″E
15	Sadras Beach	S15	12°31′2.09″N	80°9′55.62″E
16	Koovathur Beach	S16	12°25′7.71″N	80°7′54.66″E
17	Paramankeni Beach	S17	12°21′50.11″N	80°4′47.53″E
18	Marie Beach	S18	12°18′1.9794″N	80°1′57.58″E
19	Thirtavari Beach	S19	12°11′0.21″N	79°58′18.70″E
20	Anumanthai Kuppam Beach	S20	12°7′15.28″N	79°55′17.11″E
21	Kalapet Beach	S21	12°0′53.50″N	79°51′41.15″E

inserting known-energy gamma sources, ^{137}Cs (662 keV) and ^{60}Co (1173–1332 keV), into the detector.

Considering that ^{238}U, and ^{232}Th, as well as their decay products, are in secular equilibrium, the concentration of ^{238}U, and ^{232}Th were calculated from their progeny photopeak of 1764 keV for ^{214}Bi and 2614 keV for ^{208}Tl were used for determining the activity concentrations of ^{238}U and ^{232}Th respectively, and the gamma-ray transition of 1460 keV was used to determine ^{40}K concentrations. A similar geometry was maintained for counting and standard sample analysis and the counting time for all the samples was 10,000 s.

Pearson correlation analysis

Correlation analysis was performed as a bivariate statistic to identify the mutual linkages and strength of association between two variables using the linear Pearson correlation coefficient (r). It is a number between -1 and 1 that measures the strength and direction of the relationship between two variables. The statistical software IBM-SPSS version 20 was used to perform Pearson's correlation analysis among radioactive variables [22] and the ORIGIN PRO (v2022) was used for graphing analysis.

Results and discussion

Distribution of activity concentration of ^{238}U, ^{232}Th, and ^{40}K in sediments

The specific activity of ^{238}U, ^{232}Th, and ^{40}K for the collected sediment samples is determined using the following formula [33],

$$A = \frac{NCPS}{W \times \eta} \quad (1)$$

where A is the activity concentration of radionuclide (^{238}U, ^{232}Th, and ^{40}K) which is typically expressed in Becquerel per kilogram (Bq/kg), NCPS represents the total gross counts of corresponding photo peak from the spectrum subtracted from background counts and divided by counting time i.e., 10,000 s. W represents the total mass of each sample in (kg). η denotes the photo peak's efficiency as determined via efficiency calibration. In the present work, the activity concentration of ^{238}U, ^{232}Th, and ^{40}K was measured for sediment samples using NaI(Tl) detector and given in Table 2 with their respective uncertainties ($\pm 2\sigma$). As can be seen from Table 2, except for four (S6, S7, S11, and S16), all other sediment samples show a high concentration of ^{238}U in the study area. This may be due to uranium mobility [34]. Therefore, uranium migrates sequentially in the study area. On the other hand, the concentration of ^{232}Th, and ^{40}K seem to be homogeneously distributed all sampling points. The high activity concentration of ^{238}U and ^{232}Th (87 ± 3 Bq kg^{-1} and 129 ± 3 Bq kg^{-1}) was found at Thazhankuppam Beach (S2), while ^{40}K activity (692 ± 10 Bq kg^{-1}) was also high at Thiruvottiyur Beach (S3). These high activity concentrations are mainly due to their geochemical origin and they could be related to geological conditions or other factors such as rainfall, temperature, and human activities in the studied location [35]. At the same time, the existence of black sands (Fig. 2) found in these locations, which are rich in a phosphate mineral that is predominantly reddish-brown in colour and includes rare-earth elements (Ce, La, Nd, Th) PO_4, which contains a considerable level of ^{232}Th [36]. The enrichment arises because monazite's specific gravity permits it to concentrate along beaches where lighter elements are washed away [37]. Figure 3 shows the distribution of activity concentration for ^{238}U, ^{232}Th, and ^{40}K in the sediment samples.

It is clear that the activity concentration of ^{238}U, ^{232}Th, and ^{40}K increased from Kalanji Beach (S1) to Thazhankuppam Beach (S2) in the study area. However, the ^{238}U, ^{232}Th, and ^{40}K concentrations ranged from 22 ± 2 to 87 ± 3 Bq kg^{-1} with an average value of 50 Bq kg^{-1}, BDL to 129 ± 3 Bq kg^{-1} with an average value of 32 Bq kg^{-1}, 368 ± 10 to 692 ± 10 Bq kg^{-1} with an average value of 543 Bq kg^{-1} respectively. The mean activity concentrations of ^{238}U, ^{232}Th, and ^{40}K in the sediment samples are higher than the world average value [38]. This could be due to weathering of parent rock materials or anthropogenic activities like fishermen, tourists, and effluents from industries. Moreover, the contamination due to these activities may hold radioactive materials which are significantly deposited in the sediment samples.

In addition, the mean activity concentration of the radionuclides is compared with previous studies [6, 20, 39–51] with other coastal areas across the world and given in Table 3. From this comparison table, in the present study, the mean concentration of ^{238}U is significantly lower than the Penang from Malaysia [46], Preta beach of Brazil [47], while the mean ^{232}Th concentration is higher than Patras Coast of Greece [41], Red Sea from Saudi Arabia [44] and Sudan [45], Xiamen Island from China [6]. Similarly, the activity concentration of ^{40}K is lower than the Southern Coast from Albania [39], Tyrrhenian Sea of Italy [43], and Penang from Malaysia [46]. Hence, the distribution of ^{238}U and ^{40}K is homogeneous and ^{232}Th is inhomogeneous along the coastal area of North Chennai to Pondicherry, India.

Evaluation of radiological parameters

The standard radiological parameters are essential to assess the potential ecological risk and also human health risks, once the radiation is absorbed by living organisms

Table 2 Complete activity concentrations and radiological parameters associated with radionuclides ^{238}U, ^{232}Th, and ^{40}K

Sample ID	Activity concentrations (Bq kg^{-1})			Radium equivalent activity (Bq kg^{-1})	γ absorbed dose rate (nGy h^{-1})	Annual outdoor effective dose equivalent (mSv)	External hazard index	Excess lifetime cancer risks × 10^{-3} $mSvy^{-1}$	Annual gonadal dose equivalent (μSv y^{-1})
	^{238}U	^{232}Th	^{40}K						
S1	58 ± 3	125 ± 3	546 ± 11	279 ± 15	235 ± 7	0.29 ± 0.008	0.75 ± 0.02	1.01 ± 0.03	873 ± 25
S2	87 ± 3	129 ± 3	623 ± 10	319 ± 15	272 ± 6	0.33 ± 0.008	0.86 ± 0.02	1.17 ± 0.03	1002 ± 24
S3	59 ± 2	29 ± 2	692 ± 10	154 ± 14	142 ± 6	0.17 ± 0.007	0.42 ± 0.02	0.61 ± 0.02	522 ± 21
S4	47 ± 2	55 ± 3	492 ± 10	163 ± 14	143 ± 6	0.18 ± 0.007	0.44 ± 0.02	0.61 ± 0.03	529 ± 22
S5	42 ± 2	BDL	571 ± 10	86 ± 13	85 ± 5	0.10 ± 0.007	0.23 ± 0.02	0.36 ± 0.02	308 ± 20
S6	22 ± 2	21 ± 3	457 ± 10	87 ± 14	80 ± 6	0.10 ± 0.007	0.23 ± 0.02	0.34 ± 0.03	297 ± 21
S7	24 ± 2	15 ± 3	539 ± 10	87 ± 14	82 ± 6	0.10 ± 0.007	0.24 ± 0.02	0.35 ± 0.03	308 ± 21
S8	53 ± 2	27 ± 3	500 ± 10	130 ± 14	119 ± 6	0.15 ± 0.007	0.35 ± 0.02	0.51 ± 0.02	434 ± 21
S9	37 ± 2	12 ± 2	668 ± 10	106 ± 13	102 ± 6	0.12 ± 0.007	0.29 ± 0.02	0.44 ± 0.02	376 ± 20
S10	64 ± 2	10 ± 3	681 ± 10	131 ± 14	125 ± 6	0.15 ± 0.007	0.35 ± 0.02	0.54 ± 0.03	453 ± 22
S11	22 ± 2	16 ± 2	630 ± 10	93 ± 13	88 ± 6	0.11 ± 0.007	0.25 ± 0.02	0.38 ± 0.02	332 ± 20
S12	48 ± 2	42 ± 3	480 ± 10	144 ± 14	128 ± 6	0.16 ± 0.007	0.39 ± 0.02	0.55 ± 0.03	472 ± 21
S13	67 ± 3	35 ± 3	557 ± 11	161 ± 15	146 ± 6	0.18 ± 0.008	0.43 ± 0.02	0.62 ± 0.03	530 ± 23
S14	36 ± 2	BDL	517 ± 10	76 ± 13	75 ± 6	0.09 ± 0.007	0.21 ± 0.02	0.32 ± 0.02	274 ± 21
S15	65 ± 2	69 ± 3	495 ± 10	202 ± 14	176 ± 6	0.22 ± 0.007	0.54 ± 0.02	0.75 ± 0.03	644 ± 22
S16	23 ± 2	BDL	577 ± 10	68 ± 14	68 ± 6	0.08 ± 0.007	0.18 ± 0.02	0.29 ± 0.02	254 ± 21
S17	58 ± 2	14 ± 3	443 ± 10	113 ± 14	105 ± 6	0.13 ± 0.007	0.30 ± 0.02	0.45 ± 0.03	378 ± 22
S18	58 ± 2	10 ± 2	585 ± 10	117 ± 13	111 ± 6	0.14 ± 0.007	0.32 ± 0.02	0.48 ± 0.02	404 ± 20
S19	75 ± 3	15 ± 3	475 ± 10	132 ± 14	123 ± 6	0.15 ± 0.008	0.36 ± 0.02	0.53 ± 0.03	442 ± 22
S20	46 ± 2	22 ± 3	499 ± 10	117 ± 14	107 ± 6	0.13 ± 0.007	0.32 ± 0.02	0.46 ± 0.03	393 ± 22
S21	52 ± 3	21 ± 3	368 ± 10	111 ± 14	101 ± 6	0.12 ± 0.007	0.30 ± 0.02	0.43 ± 0.03	366 ± 22
Mean value	50	32	543	137	124	0.15	0.37	0.53	457
World recommended value	35	30	400	370	59	1	1	0.29 × 10^{-3}	300
BDL values	8	8	30	–	–	–	–	–	–

BDL Below detectable limit

Fig. 2 The existence of black sands in each location along the study area

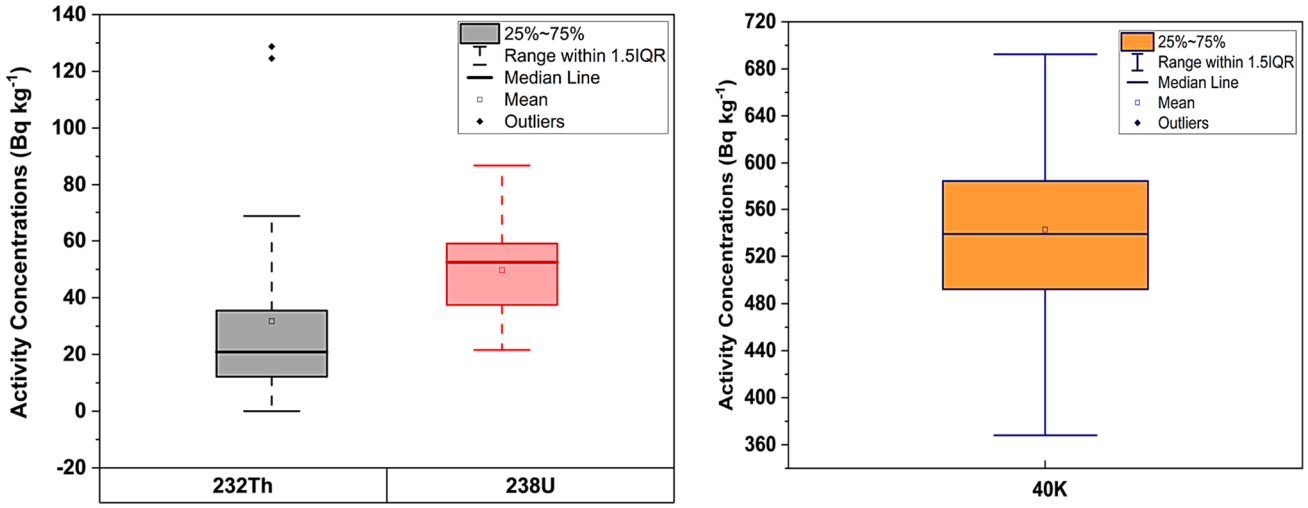

Fig. 3 Box plot showing the distribution of activity concentrations for ^{238}U, ^{232}Th, and ^{40}K in the sediment samples

Table 3 Comparison of activity concentrations of the present study with similar studies in the world

Country	Location	Activity concentrations (Bq kg^{-1})			References
		^{238}U	^{232}Th	^{40}K	
Albania	Southern Coast	27	40	550	[39]
Egypt	Red Sea	24.6	31.4	428	[40]
Ghana	Greater Accra	34	30	320	[20]
Greece	Patras coast	21.8	24.5	497	[41]
Iran	Caspian Sea	61	49	537	[42]
Italy	Tyrrhenian Sea	28.2	91.7	603.7	[43]
Saudi Arabia	Red Sea	35.46	0.92	34.34	[44]
Sudan	Red Sea	29.6	6.02	158.4	[45]
Malaysia	Penang	184	165	835	[46]
Brazil	Preta beach	239	121	110	[47]
China	Xiamen Island	14.6*	10.9	396.4	[6]
Turkey	Black sea coast	4.41–14.04	2.62–16.55	11.60–513.32	[48]
Thailand	Upper gulf	44	59	463	[49]
Spain	Northeast Coast	5–19	5–44	136–1087	[50]
Sri Lanka	West Coast	BDL-1243	14–6257	BDL-644	[51]
India	North Chennai—Pondicherry	50	32	543	Present study

*^{226}Ra

or people. The significant radiological parameters such as Ra_{eq}, D_R, AEDE, H_{ex}, ELCR, and AGDE are calculated in the sediments samples, and obtained results are compared with the international recommended value given by UNSCEAR [38] and ICRP [52]. For all calculations carried out in this section, we have used the symbols: A_U, A_{Th}, and A_K to represent the activity concentrations of ^{238}U, ^{232}Th, and ^{40}K radionuclides respectively.

Radium equivalent activity (Bq kg^{-1})

In order to express the activity levels of ^{238}U, ^{232}Th, and ^{40}K by a single quantity that takes into consideration the radiation risks associated with them, a common radiological index has been developed based on the presumption 10 Bq kg^{-1} of ^{226}Ra, 7 Bq kg^{-1} of ^{232}Th, and 130 Bq kg^{-1} of ^{40}K produce the same gamma dose rates [53–56]. The elevated concentrations of radium isotopes in sediments

can enhance the high radium equivalent activity (Ra_{eq}), which causes harmful effects on marine organisms and human health if they are exposed to gamma radiation over an extended period of time. Also, it can be used to assess whether the radium activity in the sediment is within a safe level or not, as determined by regulatory standards. The Ra_{eq} activity is mathematically defined as follows [54],

$$Ra_{eq} = A_U + 1.43A_{Th} + 0.077A_K \quad (2)$$

The Ra_{eq} values are calculated and given in Table 2. The radium equivalent activity (Ra_{eq}) in the sediment samples ranges from 68 ± 14 to 319 ± 15 Bq kg^{-1} with a mean value of 137 Bq kg^{-1} in sediment samples. As seen from Table 2, the highest Ra_{eq} was 319 Bq kg^{-1} observed at only one location S2 (Thazhankuppam Beach) where sediments are contaminated due to harbour activities. However, the obtained average value seems to be less than the recommended maximum value of 370 Bq kg^{-1} [28, 57]. Therefore, regular monitoring of radium equivalent activity is essential in these coastal sediments, which can help to ensure the safety of the people who are living in the study area.

γ-absorbed dose rate (D_R)

In order to provide a characteristics of external gamma radiation, it is necessary to calculate the absorbed dose rate for sediments above the ground surface in the study area. The conversion coefficients for calculating outdoor absorbed gamma dose rate (D_R) in the air per unit activity concentration in Bq kg^{-1} (dry weight) are 0.92 $nGyh^{-1}$ for ^{238}U, 1.1 $nGyh^{-1}$ for ^{232}Th, and 0.0807 $nGyh^{-1}$ for ^{40}K. The absorbed gamma dose rate was calculated for all locations using Eq. 3 given by UNSCEAR as follows [38, 52].

$$D_R = 0.92A_U + 1.1A_{Th} + 0.0807A_K \quad (3)$$

The calculated values of the absorbed dose rate for sediments are given in Table 2. From obtained results of Table 2, the lowest dose rate was 68 ± 6 $nGyh^{-1}$ for the sediments of Koovathur Beach represented by sample S16, while the highest dose rate was 272 ± 6 $nGyh^{-1}$ for the sediments of Thazhankuppam Beach represented by sample S2. The mean value was 124 $nGyh^{-1}$ which is greater than the global average value of 59 $nGyh^{-1}$ [38]. In addition to that, all studied locations possess a higher value of gamma dose rate and it may be due to the significant amount of uranium and thorium in the samples. These high levels of gamma absorbed dose rate in sediment can pose a significant health risk to the environment and human population living near or working with the sediments. Figure 4. Shows the variation of absorbed dose rate in the samples.

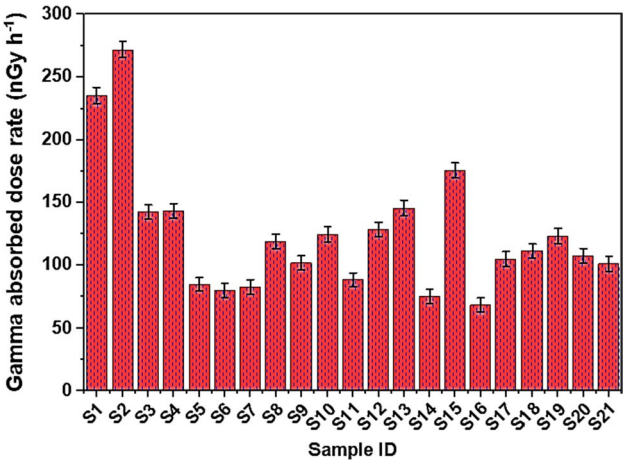

Fig. 4 Variation of the gamma absorbed dose rate in the study area

Annual effective dose equivalent (AEDE)

An outdoor annual effective dose equivalent was calculated for sediment samples by using the conversion factor of 0.7 Sv Gy^{-1} and outdoor occupancy factor (20%) to convert the total absorbed gamma dose rate in the air to the human effective dose equivalent [58]. The annual effective dose equivalent in the unit of (mSv) was calculated by the following equation:

$$AEDE_{out}(mSv) = D_R\left(nGyh^{-1}\right) \times 8760\ h \times 0.2 \times 0.7\ SvGy^{-1} \times 10^{-6} \quad (4)$$

The mean computed annual effective dose equivalent value is 0.15 mSv for collected samples, which is greater than the world average value of 0.07 mSv [38]. From obtained results, it is clearly indicated that the AEDE of all sampling locations has less than the recommended limit of 1 mSv of radiation exposure to the population [52]. Hence the emission of gamma radiation and exposure to the human population in the study area are insignificant due to the presence of ^{238}U, ^{232}Th, and ^{40}K.

External hazard index (H_{ex})

The external hazard index was proposed by Krieger [59] to ensure the harmful effects on marine biota and human populations due to natural radionuclides in the sediment samples. Therefore, the risk of gamma radiation from the environment and health effects from the activity concentration of radionuclides present in the sediment sample was assessed using the external hazard index which is calculated using the following equation [60, 61],

$$H_{ex} = \frac{A_U}{370\left(Bq\ kg^{-1}\right)} + \frac{A_{Th}}{259\left(Bq\ kg^{-1}\right)} + \frac{A_K}{4810\left(Bq\ kg^{-1}\right)} \quad (5)$$

According to the UNSCEAR report [38], the H_{ex} value of all the sampling points must be less than unity for safe from radiation exposure of humans. The calculated external hazard index for these sediment samples is given in Table 2. It is noticed that H_{ex} value of sample S1(Kalanji Beach) is 0.75 ± 0.02 and sample S2 (Thazhankuppam Beach) is 0.86 ± 0.02. These two locations show the nearest to the recommended limit of unity due to significant activity concentration of ^{238}U and ^{232}Th in these samples. However, the lowest value 0.18 of H_{ex} was noted at the sampling location of Koovathur Beach (S16), while the highest value 0.86 was observed at the sampling location of Thazhankuppam Beach (S2), with a mean value of 0.37. This mean value is less than the recommended limit of 1. Hence, the sediments in the study area may do not harm to biota, fishermen, tourists and people who are living in this region.

Excess lifetime cancer risk (ELCR)

Humans have a risk of getting cancer due to long-term exposure of even low doses of ionizing radiation from natural radionuclides in the sediment samples. The risk of cancer increases as the dose of radiation increases [62]. According to the National Cancer Institute report [63], 33% of the population will get some type of cancer during any stage of their lifetime. Hence, the additional risk parameter ELCR was calculated using Eq. 6 [64],

$$ELCR_{outdoor} = AEDE_{outdoor} \times LE \times RF \quad (6)$$

In this equation, LE stands for average life expectancy (70 years), and RF stands for risk factors such as deadly cancer risk (per sievert). In the case of stochastic effects, the International Commission on Radiological Protection (ICRP) recommends RF level is 0.05 to the public [52]. As seen from Table 2, the ELCR value of S1($1.01 \times 10^{-3} \pm 0.03$ $mSvy^{-1}$) and S2 ($1.17 \times 10^{-3} \pm 0.03$ $mSvy^{-1}$) are nearly 4 times greater than the world average value of 0.29×10^{-3} $mSvy^{-1}$ due to presence of a high concentration of ^{238}U, and ^{232}Th in the sediment samples. It is observed that a similar world average value is found in only one sample S16 and the other samples show nearly two times greater than the world average value. This may be due to the deposition of heavy minerals-rich black sands in the study area (Fig. 2).

Though, this study reveals that the minimum value was found in sample S16 (Koovathur Beach) and the maximum value was found in S2 (Thazhankuppam Beach) with a mean value of 0.53×10^{-3} $mSvy^{-1}$ as shown in Table 2. This mean value is greater than the world average value but less than the high background radiation area (HBRA) of Kerala reported by Ramasamy et al. [8] and more or less equal to Kirklareli region, Turkey reported by Taskin et al. [65]. Therefore, continuous assessment of cancer risk is necessary for the study area to protect the human population from gamma-ray exposure due to natural radioactivity.

Annual gonadal dose equivalent (AGDE)

A high (AGDE) concentration in the gonads causes negative health problems, so it is appropriate to measure the annual gonadal dose (AGDE) concentration in ^{238}U, ^{232}Th, and ^{40}K. UNSCEAR [38] considers the thyroid, lungs, female breast, gonads, active bone marrow, and bone surface cells to be the organs of interest. Hence, the annual gonadal dose equivalent (AGDE, $\mu Sv\ y^{-1}$) was calculated due to activity concentration of ^{238}U, ^{232}Th, and ^{40}K using the following equation,

$$AGDE\left(\mu Sv\ y^{-1}\right) = 3.09A_U + 4.18A_{Th} + 0.314A_K \quad (7)$$

It is particularly noted that the AGDE value of S14 and S16 is less than the world average value of 300 $\mu Sv\ y^{-1}$ due to the absence of ^{232}Th in these samples. This is clearly indicating that there is not much black sand deposition in these two locations. On the other hand, a high value of AGDE is found in samples S1 and S2 due to the significant concentration of uranium and thorium. However, the AGDE value for all other samples shows slightly greater than the world average value [62]. These elevated levels of AGDE are also known to affect the bone marrow that produces red blood cells. This may lead to cancer of the blood called leukaemia, which is often fatal. Therefore, it is necessary to study the various biological effects of ionizing radiation due to natural radionuclides in the sediment samples.

Pearson's correlation coefficient analysis

The activity concentration of radionuclides can be affected by a number of factors such as the geological composition of the sediments, the composition of minerals, and the chemical behaviour of radionuclides. Pearson correlation coefficient matrix between radionuclides (^{238}U, ^{232}Th, ^{40}K) and radiological parameters (Ra_{eq}, D_R, AEDE, H_{ex}, ELCR, and AGDE) in sediments was measured and given in Table 4. In this study, the terms strong, moderate, and weak correlation coefficients refer to > 0.70, 0.70–0.50, and 0.50–0.36 respectively were identified at $p < 0.05$ for samples (n = 21).

The obtained results show a moderate correlation between ^{232}Th and ^{238}U in the samples with an '*r*'-value of 0.527 (Fig. 5). This indicates that the ^{232}Th decay series and the ^{238}U decay series have a significant link and co-occur in sediment samples. ^{40}K has a very weak correlation between ^{238}U and ^{232}Th ($r = 0.039$ and $r = 0.027$) respectively. Hence it indicates that ^{40}K occurs in different decay

Table 4 Pearson correlation matrix among the variables in the samples

Correlations									
	^{238}U	^{232}Th	^{40}K	Ra_{eq}	D_R	AEDE	H_{ex}	ELCR	AGDE
^{238}U	1								
^{232}Th	**0.527**	1							
^{40}K	0.039	0.027	1						
Ra_{eq}	**0.715**	**0.965**	0.135	1					
D_R	**0.738**	**0.951**	0.167	**0.999**	1				
AEDE	**0.736**	**0.952**	0.166	**0.999**	**1.000**	1			
H_{ex}	**0.715**	**0.965**	0.135	**1.000**	**0.999**	**0.999**	1		
ELCR	**0.738**	**0.951**	0.167	**0.999**	**1.000**	**1.000**	**0.999**	1	
AGDE	**0.720**	**0.957**	0.173	**0.999**	**1.000**	**1.000**	**0.999**	**1.000**	1

Ra_{eq}—Radium equivalent activity, D_R—Dose rate, AEDE—Annual effective dose equivalent, H_{ex}—External hazard index, ELCR—Excess lifetime cancer risk, AGDE—Annual gonadal dose equivalent, Bold values in the table represent the strong correlation between the variables

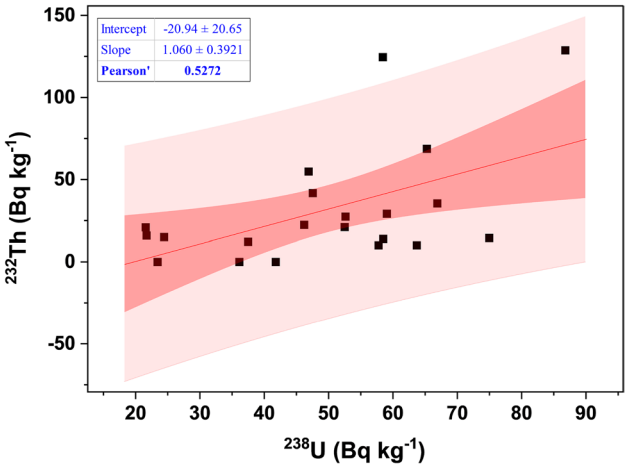

Fig. 5 Correlation between ^{232}Th and ^{238}U activity in the samples

series in nature. As seen from Table 4, all the radiological parameters strongly correlate with ^{238}U and ^{232}Th whereas a weak correlation with ^{40}K. This clearly suggested that natural radioactivity in the beach sediments is due to presence of uranium and thorium. The contribution of ^{40}K is insignificant in the samples.

Conclusion

Determination of activity concentration of ^{238}U, ^{232}Th, ^{40}K and the associated radiation hazards were carried out for sediment samples collected from North Chennai to Pondicherry coastal area, India using gamma-ray spectrometry. From obtained results, the main observation is high activity concentration and significant radiological hazards are found in samples S1 (Kalanji Beach) and S2 (Thazhankuppam Beach) due to the deposition of black sands. Also, the mean activity of ^{238}U, ^{232}Th, and ^{40}K is greater than the world average value. This may be attributed to tourists, fishermen, harbour, and industrial activities. The significant correlation of all the radiological parameters with ^{238}U, and ^{232}Th implies that, exposure of radiation is due to only uranium and thorium. The contribution of ^{40}K is insignificant in the study area. Also, radium equivalent activity, annual effective dose equivalent, and external hazard index are less than the world-recommended limit for all the studied samples. Hence, the study area doesn't possess any radiological hazards to human populations.

Author contribution V. Sathish: Conceptualization, Investigation, Software, Validation, Formal analysis, Data Curation, Writing—Original Draft. A. Chandrasekaran: Conceptualization, Methodology, Resources, Writing—Review & Editing, Visualization, Supervision.

Declarations

Conflict of interest The authors declare that there is no conflict of interest.

References

1. Vaiserman A, Koliada A, Zabuga O, Socol Y (2018) Health impacts of low-dose ionizing radiation: current scientific debates and regulatory issues. Dose-Response 16(3):1559325818796331. https://doi.org/10.1177/1559325818796331
2. Kobya Y, Taşkın H, Yeşilkanat CM, Varinlioğlu A, Korcak S (2015) Natural and artificial radioactivity assessment of dam lakes sediments in Çoruh River. Turkey J Radioanal Nucl Chem 303(1):287–295. https://doi.org/10.1007/s10967-014-3420-7
3. Lu X, Chao S, Yang F (2014) Determination of natural radioactivity and associated radiation hazard in building materials used in Weinan, China. Radiat Phys Chem 99:62–67. https://doi.org/10.1016/j.radphyschem.2014.02.021
4. Verde GL, Artiola V, D'Avino V, Commara ML, Panico M, Polichetti S, Pugliese M (2021) Measurement of natural

radionuclides in drinking water and risk assessment in a volcanic region of Italy. Water 13(22):3271. https://doi.org/10.3390/w13223271
5. Chernysh Y, Yakhnenko O, Chubur V, Roubík H (2021) Phosphogypsum recycling: a review of environmental issues, current trends, and prospects. Appl Sci 11(4):1575. https://doi.org/10.3390/app11041575
6. Huang Y, Lu X, Ding X, Feng T (2014) Natural radioactivity level in beach sand along the coast of Xiamen Island. China Mar Pollut Bull 91(1):357–361. https://doi.org/10.1016/j.marpolbul.2014.11.046
7. Chandrasekaran S, Sankaran Pillai G, Baskaran R, Venkatraman B (2019) Uncertainty evaluation in dose assessment due to spatial distribution of norm in beach sands of southeast coast of India: a probabilistic approach. Radiat Prot Dosim 187(4):482–498. https://doi.org/10.1093/rpd/ncz189
8. Ramasamy V, Sundarrajan M, Paramasivam K, Meenakshisundaram V, Surresh G (2013) Assessment of spatial distribution and radiological hazardous nature of radionuclides in high background radiation area, Kerala. India Appl Radiat Isot 73:21–31. https://doi.org/10.1016/j.apradiso.2012.11.014
9. Hassanpour N, Changizi V, Gholami M (2021) Measuring track density of alpha particles emitted from human teeth and assess of the resulting cancer risk. Int J Radiat Res. 19(3):607–613. https://doi.org/10.18869/acadpub.ijrr.19.3.607
10. Awad M, El Mezayen AM, El Azab A, Alfi SM, Ali HH, Hanfi MY (2022) Radioactive risk assessment of beach sand along the coastline of Mediterranean Sea at El-Arish area, North Sinai. Egypt. Mar. Pollut. Bull. 177:113494. https://doi.org/10.1016/j.marpolbul.2022.113494
11. Malain D, Regan PH, Bradley DA, Matthews M, Santawamaitre T, Al-Sulaiti HA (2010) Measurements of NORM in beach sand samples along the Andaman coast of Thailand after the 2004 tsunami. Nucl. Instrum. Methods Phys. Res. Sect. 619(1–3):441–445. https://doi.org/10.1016/j.nima.2009.11.047
12. Al-Trabulsy HA, Khater AEM, Habbani FI (2011) Radioactivity levels and radiological hazard indices at the Saudi coastline of the Gulf of Aqaba. Radiat Phys Chem 80(3):343–348. https://doi.org/10.1016/j.radphyschem.2010.09.002
13. Malain D, Regan PH, Bradley DA, Matthews M, Al-Sulaiti HA, Santawamaitre T (2012) An evaluation of the natural radioactivity in Andaman beach sand samples of Thailand after the 2004 tsunami. Appl Radiat Isot 70(8):1467–1474. https://doi.org/10.1016/j.apradiso.2012.04.017
14. Tari M, Zarandi SAM, Mohammadi K, Zare MR (2013) The measurements of gamma-emitting radionuclides in beach sand cores of coastal regions of Ramsar, Iran using HPGe detectors. Mar Pollut Bull 74(1):425–434. https://doi.org/10.1016/j.marpolbul.2013.06.030
15. Özmen SF, Cesur A, Boztosun I, Yavuz M (2014) Distribution of natural and anthropogenic radionuclides in beach sand samples from Mediterranean Coast of Turkey. Radiat Phys Chem 103:37–44. https://doi.org/10.1016/j.radphyschem.2014.05.034
16. Eke C, Boztosun I (2015) Determination of activity concentration of natural and artificial radionuclides in sand samples from mediterranean coast of Antalya in Turkey. Kerntechnik 80(3):280–290. https://doi.org/10.3139/124.110474
17. Abdel-Halim AA, Saleh IH (2016) Radiological characterization of beach sediments along the Alexandria-Rosetta coasts of Egypt. J Taibah Univ Sci 10(2):212–220. https://doi.org/10.1016/j.jtusci.2015.02.016
18. Darabi-Golestan F, Hezarkhani A, Zare MR (2017) Assessment of ^{226}Ra, ^{238}U, ^{232}Th, ^{137}Cs and ^{40}K activities from the northern coastline of Oman Sea (water and sediments). Mar Pollut Bull 118(1–2):197–205. https://doi.org/10.1016/j.marpolbul.2017.02.064
19. Yasmin S, Barua BS, Khandaker MU, Kamal M, Rashid MA, Sani SA, Ahmed H, Nikouravan B, Bradley DA (2018) The presence of radioactive materials in soil, sand and sediment samples of Potenga sea beach area, Chittagong, Bangladesh: Geological characteristics and environmental implication. Results Phys 8:1268–1274. https://doi.org/10.1016/j.rinp.2018.02.013
20. Botwe BO, Schirone A, Delbono I, Barsanti M, Delfanti R, Kelderman P, Nyarko E, Lens PNL (2019) Radioactivity concentrations and their radiological significance in sediments of the Tema Harbour (Greater Accra, Ghana). J Radiat Res Appl Sci 10(1):63–71. https://doi.org/10.1016/j.jrras.2016.12.002
21. Akpan AE, Ebong ED, Ekwok SE, Eyo JO (2020) Assessment of radionuclide distribution and associated radiological hazards for soils and beach sediments of Akwa Ibom Coastline, southern Nigeria. Arab J Geosci 13:753. https://doi.org/10.1007/s12517-020-05727-7
22. Shahrokhi A, Adelikhah M, Chalupnik S, Kovács T (2021) Multivariate statistical approach on distribution of natural and anthropogenic radionuclides and associated radiation indices along the north-western coastline of Aegean Sea, Greece. Mar Pollut. Bull. 163:112009. https://doi.org/10.1016/j.marpolbul.2021.112009
23. Thangam V, Rajalakshmi A, Chandrasekaran A, Arun B, Viswanathan S, Venkatraman B, Bera S (2022) Determination of natural radioactivity in beach sands collected along the coastal area of Tamilnadu, India using gamma ray spectrometry. J Radioanal Nucl Chem 331(3):1207–1223. https://doi.org/10.1007/s10967-022-08193-5
24. Devendran AA, Lakshmanan G (2019) Analysis and prediction of urban growth using neural-network-coupled agent-based cellular automata model for Chennai Metropolitan Area, Tamil Nadu, India. J Indian Soc Remote Sens 47(9):1515–1526. https://doi.org/10.1007/s12524-019-01003-8
25. ManikandaBharath K, Natesan U, Chandrasekaran S, Srinivasalu S (2022) Determination of natural radionuclides and radioactive minerals in urban coastal zone of South India using Geospatial approach. J Radioanal Nucl Chem 331(5):2005–2018. https://doi.org/10.1007/s10967-022-08284-3
26. Sundar K, Vidya R, Mukherjee A, Chandrasekaran N (2010) High chromium tolerant bacterial strains from Palar River Basin: impact of tannery pollution. Res J Environ Earth Sci 2(2):112–117
27. Järvelill JI, Koch R, Raukas A, Vaasma T (2018) Hazardous radioactivity levels and heavy mineral concentrations in beach sediments of Lake Peipsi, northeastern Estonia. Geologos 24(1):1–12. https://doi.org/10.2478/logos-2018-0001
28. Sathish V, Chandrasekaran A, Manigandan S, Tamilarasi A, Thangam V (2022) Assessment of natural radiation hazards and function of heat production rate in lake sediments of Puliyanthangal Lake surrounding the Ranipet industrial area Tamil Nadu. J Radioanal Nucl Chem 331(3):1495–1505. https://doi.org/10.1007/s10967-022-08207-2
29. Bharath KM, Natesan U, Chandrasekaran S, Srinivasalu S, Abdelrahman K, Abu-Alam T, Abioui M (2023) Geochemometrics of primordial radionuclides and their potential radiological risk in coastal sediments of Southeast Coast of India. J Radiat. Res. Appl. Sci. 16(1):100525. https://doi.org/10.1016/j.jrras.2023.100525
30. Jananee B, Rajalakshmi A, Thangam V, Bharath KM, Sathish V (2021) Natural radioactivity in soils of Elephant hills, Tamilnadu. India J Radioanal Nucl Chem 329(3):1261–1268. https://doi.org/10.1007/s10967-021-07886-7
31. Hung NQ, Chuong HD, Thanh TT, Van Tao C (2016) Intercomparison NaI (Tl) and HPGe spectrometry to studies of natural radioactivity on geological samples. J Environ Radioact 164:197–201. https://doi.org/10.1016/j.jenvrad.2016.07.035
32. Sathish V, Chandrasekaran A, Tamilarasi A, Thangam V (2022) Natural radioactivity and mineral assessment in red and black colored soils collected from agricultural area

of Tiruvannamalai district of Tamil Nadu India. J Radioanal Nucl Chem 331(11):4513–4528. https://doi.org/10.1007/s10967-022-08570-0
33. Senthil Kumar CK, Chandrasekaran A, Harikrishnan N, Ravisankar R (2020) Measurement of ^{226}Ra, ^{232}Th and ^{40}K and the associated radiological hazards in Ponnai river sand, Tamilnadu, India using Gamma ray spectrometry. Int J Environ Anal Chem 102(17):5432–5444. https://doi.org/10.1080/03067319.2020.1796996
34. Júnior JS, Cardoso JJRF, Silva CM, Silveira SV, Amaral RS (2006) Determination of radionuclides in the environment using gamma-spectrometry. J Radioanal Nucl Chem 269:451–455. https://doi.org/10.1007/s10967-006-0417-x
35. Harb S (2008) Natural radioactivity and external gamma radiation exposure at the coastal Red Sea in Egypt. Radiat Prot Dosim 130(3):376–384. https://doi.org/10.1093/rpd/ncn064
36. Haneklaus N, Barbossa S, Basallote MD, Bertau M, Bilal E, Chajduk E, Chernysh Y, Chubur V, Cruz J, Dziarczykowski K, Fröhlich P (2022) Closing the upcoming EU gypsum gap with phosphogypsum. Resour. Conserv. Recycl. 182:106328. https://doi.org/10.1016/j.resconrec.2022.106328
37. Uosif MAM, El-Taher A, Abbady AGE (2008) Radiological significance beach sand used for climate therapy from Safaga. Egypt Radiat Prot Dosim 131(3):331–339. https://doi.org/10.1093/rpd/ncn175
38. UNSCEAR (2000) United Nations Scientifc Committee on the Effect of Atomic Radiation. Sources and Effects of Ionizing Radiation. Report to general Assembly, with Scientifc Annexes, United Nations, New York.
39. Tsabaris C, Eleftheriou G, Kapsimalis V, Anagnostou C, Vlastou R, Durmishi C, Kedhi M, Kalfas CA (2007) Radioactivity levels of recent sediments in the Butrint Lagoon and the adjacent coast of Albania. Appl Radiat Isot 65(4):445–453. https://doi.org/10.1016/j.apradiso.2006.11.006
40. El Mamoney MH, Khater AEM (2004) Environmental characterization and radioecological impacts of non-nuclear industries on the Red Sea coast. J Environ Radioact 73(2):151–168. https://doi.org/10.1016/j.jenvrad.2003.08.008
41. Papaefthymiou H, Papatheodorou G, Moustakli A, Christodoulou D, Geraga M (2007) Natural radionuclides and ^{137}Cs distributions and their relationship with sedimentological processes in Patras Harbour. Greece J Environ Radioact 94(2):55–74. https://doi.org/10.1016/j.jenvrad.2006.12.014
42. Reza Abdi M, Hassanzadeh S, Kamali M, Reza Raji H (2009) ^{238}U, ^{232}Th, ^{40}K and ^{137}Cs activity concentrations along the southern coast of the Caspian Sea. Iran Mar Pollut Bull 58(5):658–662. https://doi.org/10.1016/j.marpolbul.2009.01.009
43. Desideri D, Meli MA, Roselli C, Testa C (2002) Geochemical partitioning of actinides, ^{137}Cs and ^{40}K in a Tyrrhenian Sea sediment sample: comparison to stable elements. J Radioanal Nucl Chem 251(1):37–41. https://doi.org/10.1023/A:1015086009384
44. Al-Zahrany AA, Farouk MA, Al-Yousef AA (2012) Distribution of naturally occurring radioactivity and ^{137}Cs in the marine sediment of Farasan island, Southern Red Sea. Saudi Arabia Radiat Prot Dosim 152(1–3):135–139. https://doi.org/10.1093/rpd/ncs207
45. Sam AK, Ahamed MMO, El Khangi FA, El Nigumi YO, Holm E (1998) Radioactivity levels in the Red Sea coastal environment of Sudan. Mar Pollut Bull 36(1):19–26. https://doi.org/10.1016/S0025-326X(98)90025-X
46. Almayahi BA, Tajuddin AA, Jaafar MS (2012) Efect of the natural radioactivity concentrations and 226Ra/238U disequilibrium on cancer diseases in Penang. Malaysia Radiat Phys Chem 81(10):1547–1558. https://doi.org/10.1016/j.radphyschem.2012.03.018
47. Freitas AC, Alencar AS (2004) Gamma dose rates and distribution of natural radionuclides in sand beaches-Ilha Grande. Southeastern Brazil J Environ Radioact 75(2):211–223. https://doi.org/10.1016/j.jenvrad.2004.01.002
48. Korkulu Z, Özkan N (2013) Determination of natural radioactivity levels of beach sand samples in the black sea coast of Kocaeli (Turkey). Radiat Phys Chem 88:27–31. https://doi.org/10.1016/j.radphyschem.2013.03.022
49. Khuntong S, Phaophang C, Sudprasert W (2015) Assessment of radionuclides and heavy metals in marine sediments along the Upper Gulf of Thailand. J. Phys. Conference Series 611(1):012023. https://doi.org/10.1088/1742-6596/611/1/012023
50. Rosell JR, Ortega X, Dies X (1991) Natural and artificial radionuclides on the northeast coast of Spain. Health Phys 60(5):709–712
51. Mahawatte P, Fernando KNR (2013) Radioactivity levels in beach sand from the West Coast of Sri Lanka. J Natl Sci Found Sri Lanka 41(4):279–285. https://doi.org/10.4038/jnsfsr.v41i4.6249
52. ICRP (1991) Recommendations of the International Commission on Radiological Protection. ICRP. Publication 60, Ann. ICRP21 (1–3)
53. Diab HM, Nouh SA, Hamdy E-F (2008) Evaluation of natural radioactivity in a cultivated area around a fertilizer factory. Nucl Radiat Phys 3(1):53–62
54. Beretka J, Mathew PJ (1985) Natural radioactivity of Australian building materials, industrial wastes and byproducts. Health Phys 48:87–95
55. Organisation to Economic Cooperation and Development (OECD) (1979) Exposure to radiation from the natural radioactivity in building materials. Report by a Group of Expert of the OECD. Nuclear Energy Agency, Paris, France.
56. UNSCEAR (1982) Ionizing Radiation Sources and Biological Effect. United Nations Scientifc Committee on the Effect of Atomic Radiation (A/37/45). United Nations, New York.
57. International Atomic Energy Agency-IAEA (2003) Extent of environmental contamination by naturally occurring radioactive material (NORM) and technological options for mitigation. Technical Reports Series No. 419, STI/DOC/010/419, Vienna
58. United Nations Scientifc Committee on the Effect of Atomic Radiation UNSCEAR (2010) Sources and Effects of Ionizing Radiation. United Nations. New York
59. Krieger R (1981) Radioactivity of construction materials. Betonwerk Fertigteil Technol 47(8):468–473
60. Huda A (2011) Determination of Natural Radioactivity Levels in the State of Qatar Using High-Resolution Gamma-ray Spectrometry. Ph.D. Thesis. University of Surrey, UK.
61. Veiga R, Sanches N, Anjos RM, Macario K, Bastos J, Iguatemy M, Aguiar JG, Santos AMA, Mosquera B, Carvalho C, BaptistaFilho M (2006) Measurement of natural radioactivity in Brazilian beach sands. Radiat Meas 41(2):189–196. https://doi.org/10.1016/j.radmeas.2005.05.001
62. Senthilkumar RD, Narayanaswamy R (2016) Assessment of radiological hazards in the industrial effluent disposed soil with statistical analyses. J Radiat Res Appl Sci 9(4):449–456. https://doi.org/10.1016/j.jrras.2016.07.002
63. National Cancer Institute, USA. (2009). Surveillance, Epidemiology, and End Results (SEER) Program. The Surveillance, Epidemiology, and End Results (SEER) Program of the National Cancer Institute works to provide information on cancer statistics in an effort to reduce the burden of cancer among the U.S. population.
64. Ramasamy V, Suresh G, Meenakshisundaram V, Gajendran V (2009) Evaluation of natural radionuclide content in river

sediments and excess lifetime cancer risk due to gamma radioactivity. Res J Environ Sci 1(1):6–10
65. Taskin H, Karavus M, Ay P, Topuzoglu A, Hidiroglu S, Karahan G (2009) The investigation of radionuclide concentrations in soil and lifetime cancer risk due to gamma radioactivity in Zonguldak Turkey. J Environ Radioact 100:49–53. https://doi.org/10.1016/j.jenvrad.2008.10.012